Прилози, Одд. мат. тех. науки, МАНУ, **XXIX**, 1–2 (2008), стр. 49–67
Contributions, Sec. Math. Tech. Sci., MANU, **XXIX**, 1–2 (2008), pp. 49–67
ISSN 0351–3246
UDC: 547.313:548.5

CRYSTALLIZATION OF POLYPROPYLENE: APPLICATION OF DIFFERENTIAL SCANNING CALORIMETRY

PART I. ISOTHERMAL AND NON-ISOTHERMAL CRYSTALLIZATION

Luljeta Raka, Gordana Bogoeva-Gaceva

A b s t r a c t: Theoretical background of the crystallization of isotactic polypropylene is summarized with respect to the potential of DSC method applied for the analysis of isothermal and non-isothermal processes.

Key words: polypropylene; isotactic; crystallization behavior; isothermal crystallization; non-isothermal crystallization; differential scanning calorimetry (DSC)

1. INTRODUCTION

The subject of polymer crystallization has been of great interest for several decades due to the complex phenomena usually taking place, as well as its industrial importance [1–5].

It is generally known that physical and mechanical properties of a semi-crystalline polymer are dictated by morphology, which is influenced by crystallization behavior of the polymer. Crystallization behavior is strongly influenced by molecular characteristics (e.g. molecular mass averages, molecular mass distribution, stereo-regularity, etc) of the crystallizing polymer and the processing conditions (the rate of cooling, the presence of orientation in the melt, and the melt temperature) [6].

One of the main advances in the polyolefin technology in the last decade was the use of single-site metallocene catalysts to produce a new variety of

polyolefin. The property profile of metallocene-derived plastics is much better controllable because metallocene catalysis is homogeneous in contrast to the heterogeneous Ziegler-Natta catalysts. For that reason the metallocene products are more homogeneous in terms of stereo-regularity and the molecular mass distribution, which provide improved control of molecular mass (M_w), molecular mass distribution (MMD = M_w/M_n), and short-chain branching (SCB). Due to the uniformity of polypropylene (PP) chains, for instance, metallocene-catalyzed PP has a very narrow MMD (MMD of 2–3) compared to the conventional PP (minimum MMD of 3–6) [7].

These new generation of polymers are of great scientific interest and new technologies are being developed to establish a better morphology control. Even if the occurrence of the set of transverse crystallites for the metallocene-catalyzed PP is known, it still remains a difficult matter to analyze the crystallization and melting processes for a given sample [8]. In this sense, crystallization and melting characteristics of the metallocene-catalyzed isotactic PP (iPP) have recently attracted interest from both theoretical and practical point of view [7, 9–13].

Also, the study on formation, microstructure and morphology of β-PP has attracted a great deal of interest. The presence of high content of β-phase in iPP usually can affect mechanical properties, namely enhance the impact strength and lower stiffness of β-nucleated iPP, which is of considerable importance from the viewpoint of industrial application [14].

Investigation of the crystallization behavior of polypropylene has become a subject of special interest also due to the increased development of some new technologies, where semi-crystalline thermoplastic polymers are used as matrices for long fiber-reinforced composite materials [15–18]. The morphology and the resulting crystallinity of the thermoplastic component in composite material may be significantly influenced by the condition (temperature regime, pressure, etc) applied during processing. On the other hand, the degree of crystallinity and morphology of the matrix may affect the mechanical properties of the composite material [19, 20].

However, due to its nonpolar nature, the use of homo-iPP in composite materials, in which the bonding between the fibers and the polymer matrix strongly affect the overall composite properties, is limited. So, different methods of chemical modification of PPs are developed to improve compatibility with and the adhesion to the reinforcing fibers. The grafting of different monomers, such as acrylic and methacrylic acids, acrylamide, ethylene glycol

methacrylate as well as maleic anhydride (MAH), offers improved adhesion to numerous filler and decreased critical tension, introducing polar functional groups into the polymer backbone without affecting the basic properties of the polymer [21–23].

Extensive research has shown that the morphology of iPP as well as its crystallization and melting behavior are affected by the presence of reinforcing fibers (carbon, glass, PET, PI, etc.) and different fillers (nanoparticles)**.** The presence of a solid surface (substrate) in contact with thermoplastic polymers during crystallization from the melt generally favors the heterogeneous nucleation [24, 25] and often a growth of the transcrystalline zone, a special type of oriented morphology at the substrate/matrix interface under proper condition. This specific morphology of the polymer in the transcrystalline zone, which has a great technological importance, is expected to influence the adhesion at the interface, due to an increased nucleation density as well as the mechanical properties of the interface due to a preferential orientation of the lamellae [26, 27].

2. THEORETICAL BACKGROUND

2.1. Thermodynamic considerations

The crystallization process is a first-order thermodynamic phase transition and occurs when a polymer is cooled well below its melting temperature, and the transformation that takes place can be described by a nucleation and growth. Like any phase transformation, the polymer crystallization obeys the laws of thermodynamics, which determine whether under specific circumstances, crystals can exist or not [28].

The Gibbs energy, G of any system is related to the enthalpy, H and the entropy, S by the equation:

$$G = (U + pV) - TS = H - TS \tag{1}$$

where T is the thermodynamic temperature. The system is in equilibrium when G is a minimum. A polymer melt consists of randomly coiled and entangled chains, so the entropy is much higher than if the molecules are in the form of extended chains because of the existence of many more conformations available to a coil than for a fully extended chain. The higher value of S leads to a

lower value of G. The crystallization leads to a high degree of order in polymer crystals and thus a reduction in entropy, S that is more than offset by the large reduction in enthalpy that occurs during crystallization. If the magnitude of the enthalpy change ΔH_m (latent heat) is greater than that of the product of the melting temperature and the entropy change ($T_m \Delta S_m$) crystallization will be favored thermodynamically since lower value of G will result. It can be only applied to a process, which occurs quasi-statically, that is very slowly. But when polymers are processed industrially, they are cooled rapidly from the melt, so the crystallization is controlled by the kinetics and the rate at which the crystals nucleate and grow becomes important [29].

2.2. Cold-crystallization

With many crystallizable polymers it is possible to cool the melt so rapidly that crystallization is completely absent and amorphous glassy polymer results. With these systems crystallization can normally be induced by annealing the amorphous polymer at a temperature between the glass transition temperature, T_g and the melting point, T_m of the crystals. This phenomenon is generally known as cold-crystallization.

The cold-crystallization process is suitable for studying polymers that have a high degree of aromatic character in the backbone (PET, PPS, PEEK etc.), and can exhibit a strong exotherm immediately above their glass transition temperature upon reheating. Since the energy associated with the recrystallization exotherm is strongly influenced by the rate of cooling from melt, this is yet another ”handle” for inferring the thermal history of the sample. PET is the best example of polymer where cold-crystallization occurs. Although of enormous importance from a scientific point of view, cold-crystallization has not played an important role in the technological application of polymers, since polymer processing occurs in the melt phase and it is the size, dimension and distribution of the crystallites developed upon cooling from the melt that determine the final properties of the material [1]. A number of papers have been published on this topic, so they were mainly concerned with the kinetic aspects of the process and the way it is influenced by the molecular weight, chain orientation, aging below and above T_g and by exposure to the organic solvents [30]. Supaphol and Spruiell have analyzed isothermal melt and cold-crystallization kinetics of sPP using calorimetric measurements [31].

2.3. Solution and melt-grown single crystals

A characteristic feature of solution-grown polymer crystals is that they are small when are examined in an electron microscope. The crystals are normally precipitated either by cooling a hot solution, which is the most widely used method, or by the addition of a non-solvent. Small isolated lamellar crystals are obtained from the molecules that are folded and the fold regions give rise to the non-crystalline component in the crystals. There is a higher degree of perfection in solution-grown polymer crystals than in the melt-crystalline counterparts. Measurements of the density and other properties of solution grown polymer crystals have shown that they are not perfect crystals, which means that non-crystalline material must be present in the crystal (in the fold surfaces of the crystals).

The morphology of crystals grown from the melt is different and more complex crystal forms are obtained. Spherulites are spherically symmetrical crystalline structure composed of individual lamellar crystal plates, which grow from a central nucleus. It is observed that each spherulite exhibits a characteristic Maltese cross. Usually spherulites are spherical in shape during initial stage of crystallization but during the later stages, the spherulites impinge one their neighbors. When the spherulites are nucleated simultaneously, the boundaries between them are straight. However, when the spherulites have been nucleated at different times, they are different in size when impinging on one another, their boundaries form hyperbolas [29, 32].

2.4. Flow-induced crystallization

The processing history of flow on semicrystalline polymer melt can affect the morphology, morphological distribution and product properties as well. In most polymer processing operations, both the morphology and its distribution through the resultant polymer products are strongly influenced by the orientation induced by the flow in the molten state. In particular flow-induced crystallization of polymer melts can results in the formation of a so-called shish-kebab structure in semicrystaline polymers under appropriate conditions [33–36]. This special kind of chain crystalline assembly consists of folded-chain lamellae or kebabs periodically held together by fibrillar crystals or shishes [33–43] which is a result of a coil-to-stretch transition of polymer chains in the melt crystallization when the shear rate exceeds a critical value [33, 37]. It has been predicted and observed that longer coiled-chains (longer than a critical length) of a polydisperse polymer melt can be stretch to the

shishes while at the same flow rate shorter coiled-chains epitaxially grow into the kebabs. It has been found that the flow fields are always essential for the formation of the shish, whereas the kebabs can grow on the shish in the absence of any flow [37, 39, 40].

2.5. The Hoffman-Lauritzen theory of crystal growth

Various theories have been proposed to describe the kinetics of homopolymer crystallization. The *Hoffman-Lauritzen* (HL) theory, which was put forward more than 40 years ago by Hoffman and Lauritzen [44–48], and Frank and Tosi [49], was one of the first analytical theories to illustrate how polymers crystallize. They utilized a lateral growth, surface nucleation controlled process to describe the growth rate of polymer lamellar crystals. An existing crystal with a defined atomically smooth crystallographic surface provides a growth front. Chain molecules deposit onto the growth plane and start to crystallize onto the lattice one stem at a time to form lamellae. The crystal growth rate perpendicular to the growth front is linear at a constant T_c. This kinetic model contains four parameters to describe the nucleation process: the surface nucleation rate, i; the growth rate parallel to the growth plane that covers the growth front after the surface nucleation which is called the lateral covering rate, g; the width of the growth front (the substrate length) which the nucleation and growth covers, L, and the growth rate perpendicular to the growth plane, G. The HL theory predicts three regimes, which are shown in Fig. 1 (a-c).

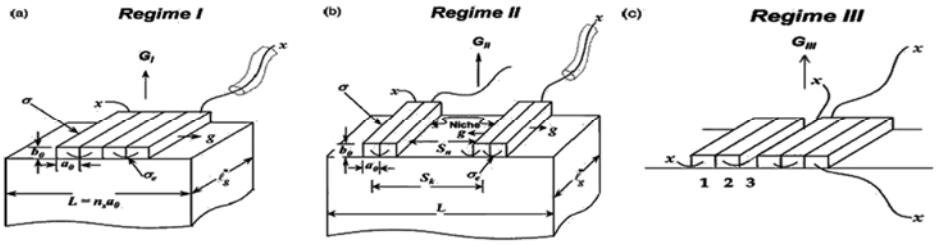

Fig. 1. Schematic drawings of how polymer crystal growth takes place in three regimes: (a) regime I; (b) regime II; and (c) regime III. The '*x*' represents chain ends [50]. (Abbreviations are given in the text)

Regime I: takes place at low ΔT when the growth from a single nucleus covers the entire growth plane L (a). The analytical expression for the growth rate in regime I is given by eq. 2 [29–31, 33–34]:

$$G_{\mathrm{I}} = b_{\mathrm{o}} iL \tag{2}$$

where b_o is the thickness of the molecular layer crystallized on the substrate, and L is the substrate length which is covered by one surface nucleus under condition that $g/L <<< iL$ [50].

Regime II: with increasing ΔT it is evident that on the substrate of width L, more than one nucleus is formed. The critical factor in this regime is the niche separation between two neighboring nuclei. At the higher end of T_{c} in regime II, the niche separation is large. As the nucleation rate increases with increasing ΔT, the niche separation is reduced. The analytical expression of the growth rate is given by:

$$G_{\mathrm{II}} = (ib_{\mathrm{o}} g)^{1/2} \tag{3}$$

Regime III: upon further decreasing the T_{c}, one passes into the lower T_{c} end of regime II resulting in changes in the crystal growth, and then, one enters regime III as shown in Fig. 1 (c). The niche separation distance reaches the same order of magnitude as the stem width a_{o}. Therefore, the lateral covering rate, g is not a dominant factor, so the analytical expression, g or the growth rate returns back to:

$$G_{\mathrm{III}} = ib_{\mathrm{o}} L' \tag{4}$$

where L' is the effective substrate length (width between two neighboring niches), which correspond to about 2–3 stem widths [50].

Thermodynamically, the rate of lateral growth should be higher than the rate of attachment of a nucleus on the growing surface, because of the lower energy penalty associated with attachment to a niche on the crystal surface. The general view is that the mobility of polymer chains is low in regime III, which occurs at temperature lower than both regimes II and I. The regime II–III transition is diffusion controlled, in contrast to the regime I–II transition, which is determined by under-cooling [51, 52].

Since then, modifications to the HL theory and suggestions for new approaches have been reported, but the core physical picture of the HL theory has largely remained intact.

For all three regimes, the overall growth rate, G is given as a function of the crystallization temperature, T_{c} by following bi-exponential equation in the context of the Lauritzen-Hoffman secondary nucleation theory [13]:

$$G = G_o \exp\left[-\frac{U^*}{R(T_c - T_\infty)}\right]\exp\left[-\frac{K_g}{T_c(\Delta T)f}\right] \tag{5}$$

where G_o is the pre-exponential factor. The first exponential term contains the contribution of the diffusion process to the growth rate, while the second exponential term is the contribution of the nucleation process. U^* denotes the activation energy which characterize the molecular diffusion across the interfacial boundary between melt and crystals. T_∞ is usually set equal to ($T_g - 30$) K, with T_g being the glass transition temperature of the polymer. K_g is a nucleation constant and ΔT denotes the degree of under cooling ($\Delta T = T_m^{\,o} - T_c$). f is a correction factor given as $f = 2T_c/(T_m^{\,o} + T_c)$. The equilibrium melting temperature $T_m^{\,o}$ can be calculated using the linear or non-linear Hoffman-Weeks extrapolation.

For a secondary or heterogeneous nucleation, K_g can be calculated from:

$$K_g = \frac{n\sigma\sigma_e b_o T_m^{\,o}}{\Delta h_f \rho_c k_B} \tag{6}$$

where n takes the value of 4 when crystallization takes place in regime I or III and the value 2 in regime II, σ and σ_e are the side surface (lateral) and fold surface free energies which measure the work required to create a new surface, b_o is the single layer thickness, $\Delta h_f \rho_c = \Delta H_f$ is the enthalpy of melting per unit volume and k_B is the Boltzmann constant [50].

The HL theory has been sufficiently fundamental in its assumption to describe major crystallization phenomena for a wide range of semi-crystalline polymers.

iPP is a favorable model substance, because its linear growth rate (G) can be determined with high precision in a wide temperature range (T_c) in term of the changes in the radii of spherulites with time. According to this theory, regime transitions are observed when the experimental function $G = f(T_c)$ is linear within a given regime if $\ln G$ corrected by a transport factor, $U^*/[R(T_c - T_\infty)]$ is plotted against $[T_c \Delta T f]^{-1}$. Break points between the linear sections refer to the transition temperatures T (I–II) and T (II–III) from one

regime to the other. The ratio of the slopes between two adjacent regimes is 2. From the slopes of the straight lines, the surface free energy of folding $\Delta\sigma_e$ can be calculated if the necessary material constants are known. From the literature data, it is shown that the experimental values of G for α PP fall in the regime II–III transition temperature 410 K, 411 K or 407–409 K and, for β-PP 406 K, which depends on molecular dynamics. The transition temperature (I–II) is 425–431 K, obtained with conventional isothermal methods when the equilibrium melting temperature T_m^o = 458.2 K was estimated by Monasse and Haudin [53, 54].

3. DIFFERENCIAL SCANNING CALORIMETRY (DSC)

Calorimetry is particularly useful study technique, which is part of a group of techniques called thermal analysis (TA). Thermal analysis is based upon the detection of changes in the heat content (enthalpy) or the specific heat of the sample with temperature.

DSC has been extensively used for measuring the actual rate of crystallization continuously in time or, under non-isothermal condition, in temperature.

Thermal transitions as a function of temperature and time give quantitative and qualitative information regarding physical (and chemical) changes such as melting, crystallization, recrystallization, glass transition temperatures, cold crystallization, polymerization, degradation reactions, volatilization or changes in heat capacity. Melting and crystallization temperatures can be determined (Fig. 2).

DSC is a commonly used technique, which is able to provide information on melting and crystallization temperature and crystallinity of iPP when heating or cooling mode is applied. In the heating mode, a PP sample (5–8 mg) is heated up from ambient temperature in the DSC furnace at a preset heating rate until it reaches its melting temperature. However, in the cooling mode there are two methods of studying the crystallization kinetics, isothermal and non-isothermal.

In the isothermal crystallization, the tested sample is first heated above its melting temperature and then rapidly quenched to the prescribed crystallization temperature so that crystallization occurs isothermally. In the non-isothermal crystallization, the tested sample is first heated to a prescribed temperature above its melting point, and then cooled at a preset cooling rate.

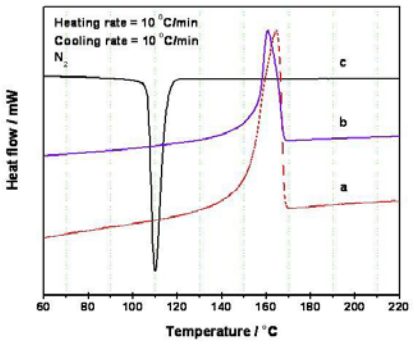

Fig. 2. DSC heating (a and b) and cooling (c) runs at 10 K/min of PP sample [55]

The degree of crystallinity of the sample, X_c at the peak melting or crystallization temperature is calculated from the enthalpy of melting or crystallization, respectively (ΔH_m or ΔH_c (J/g)) obtained from the DSC measurements (Fig. 3) by comparison with literature data for 100% crystalline iPP according to the following equation (after normalization) [56]:

$$X_c = \frac{\Delta H_m}{\Delta H^o}, \tag{7}$$

where ΔH^o is the melting enthalpy of 100 % crystalline polymer ($\Delta H^o = 207$ J/g for 100 % iPP) [53].

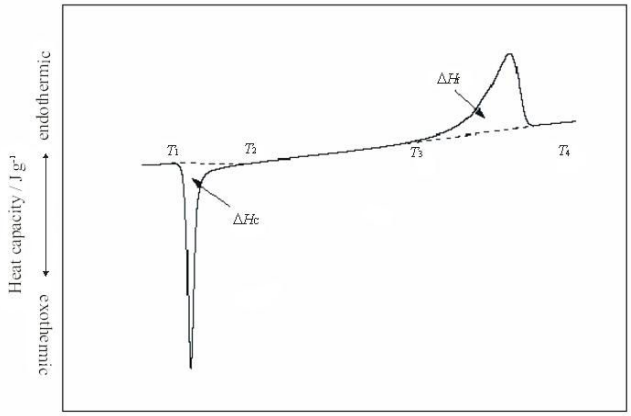

Fig. 3. Schematic representation of the enthalpy changes on heating an amorphous crystallizable polymer: cold crystallization (T_1–T_2) and melting (T_3–T_4)

From DSC curves, the values of relative crystallinity at various cooling rates can be calculated. The relative crystallinity as a function of time can be defined as:

$$X_{\mathrm{t}} = \frac{X_{\mathrm{t}}}{X_{\infty}} = \frac{\int_{t_0}^{t} (\mathrm{d}H/\mathrm{d}t)\mathrm{d}t}{\int_{t_0}^{t_{\infty}} (\mathrm{d}H/\mathrm{d}t)\mathrm{d}t} \tag{8}$$

where $(\mathrm{d}H/\mathrm{d}t)$ is the rate of heat flow, X_{t} and X_{∞} are the crystallinity at time t, and at the end of crystallization process (t_{∞}), respectively.

3.1. Isothermal crystallization kinetics

The crystallization kinetics of polymeric material under isothermal conditions for various modes of nucleation and growth can be well approximated by the known Avrami equation over a wide crystallization temperature range [57]. This equation is derived by assuming random nucleation, a constant growth rate, and a constant rate of nucleation (or constant nucleation density), and the general form of the Avrami expression is given as:

$$X = 1 - \exp(-Kt^{\mathrm{n}}) \tag{9}$$

where X is a crystal conversion; n is the Avrami exponent; and K a rate constant, which usually follows the Arrhenius relationship with temperature:

$$K = A\exp(E\mathrm{a}/RT) \tag{10}$$

where A is the pre-exponential factor, and E_{a} is the activation energy. The value of the Avrami exponent depends on the mechanism of nucleation and geometry of crystal growth, and the constant K includes nucleation parameters as well as growth-rate parameters.

Memory effects during isothermal crystallization of iPP by Ziabicki and Alfonso have been extensively studied. [58]. The effects of temperature and duration of melting on the rate of isothermal crystallization were investigated by DSC. It was found that crystallization rate decrease with increasing melt temperature and melting time, suggesting gradual destruction of predeter-

mined nuclei (clusters, crystal aggregates) with activation energy E_a = 89 ± 7 kJ/mol as a main mechanism of the observed memory effects.

DSC technique is used as well as for kinetic studies. The extent of crystallization can be recorded and the parameters of crystallization determined.

It is well known that in highly filled systems (such as fiber reinforced polymers), the original three-dimensional geometry of polymer spherulites can be reduced to two-dimensional discs or one-dimensional needles, and a lower value of growth order leads to a lower exponent *n* in the Avrami equation. Although these effects influence the assumptions in a simple Avrami process, besides for neat polymers, an Avrami plot is nevertheless widely applied to describe the crystallization kinetics in more complex polymer systems [59].

For the studied range of crystallization temperatures (121–130 ºC), values for *n* ranging from 1.9 to 3.4 for the iPPs and from 1.0 to 2.8 for the model composites (fiber reinforced iPP) were obtained. The values of the Avrami exponent depend also on the applied experimental method (dilatometry, DSC, optical microscopy) [60, 61]. Literature DSC data for the Avrami exponent varied with the temperature range from 2.0 to 3.5 [61–66]. Dilatometry data are usually close to *n* = 3.0 [67].

3.2. Non-isothermal crystallization kinetics

From dynamic crystallization experiments, data for the crystallization exotherms as a function of temperature $\mathrm{d}H_c / \mathrm{d}T$ can be obtained, for each cooling rate. Then, the relative crystallinity as a function of temperature $X(T)$ can be formulated as:

$$X(T) = \frac{\int_{T_0}^{T_c} (\mathrm{d}H_c / \mathrm{d}T)\mathrm{d}T}{\int_{T_0}^{T_\infty} (\mathrm{d}H_c / \mathrm{d}T)\mathrm{d}T} \tag{11}$$

where T_o denotes the initial crystallization temperature, T_c and T_∞ the crystallization temperature at time, *t* and after the completion of the crystallization process, respectively.

The crystallization temperature, T_c can be converted to crystallization time, t, with the well-known relationship for non-isothermal crystallization process that is strictly valid when the sample experiences the same thermal history as designed by the DSC furnace.

$$t = \frac{(T_o - T_c)}{\beta} \tag{12}$$

where β is the constant cooling rate.

To quantitatively describe the evolution of crystallinity during non-isothermal crystallization, a number of models have been proposed and the majority of these formulations are based on the Avrami equation [57]. The most common approach is Ozawa theory that extended the Avrami theory by assuming that sample was cooled with constant rate [4]. In the Ozawa method, the time variable in the Avrami equation was replaced by a cooling rate, and the relative crystallinity was derived as a function of constant cooling rate as:

$$X_t = 1 - \exp\left[-\left(K_o / \beta\right)\right]^m \tag{13}$$

where K and m are the Ozawa crystallization rate constant and the Ozawa exponent, respectively. Both of the Ozawa kinetic parameters hold similar physical meaning to those of the Avrami ones.

DSC studies of iPP crystallization at a constant cooling rate enable determination of nucleation regime by applying the Ozawa's theory, delivering results consistent with those obtained by direct microscopic observation [2].

3.3. Melting behavior

The melting of polymers is a complex process and extends over a wide temperature range since the size and structure of crystallites vary considerably. Melting of iPP is affected by many factors, such as molecular mass and molecular mass distribution, degree of isotacticity, and head to-tail sequences and the presence of different crystal forms [53]. The appearance of multiple peaks during the melting after isothermal or non-isothermal crystallization, observed by DSC analysis, is usually related to some of the following factors: existence of different crystal structures, phenomenon of recrystallization and perfection during fusion and different crystal sizes. *Petracone et al*. reported that the double

melting peaks may be attributed to existing of less-ordered α_1 and more-ordered α_2 forms with a well-defined deposition of up and down helices in the unit cells. [68–70]. Double melting peaks are observed when the crystallization is carried out at low T_c (388 K). The high-temperature melting peak gradually diminishes and finally disappears as T_c increased. The same behavior is observed in iPP/fiber model composites [23] and iPP/clay nanocomposites as shown in Fig. 4 [71]. At the same time, the value of low-temperature melting peak increases as T_c increases from 430.7 K to 435.7 K and the melting peak becomes sharper. Besides the fact that the melting and crystallization behavior of iPP are comprehensively reviewed [53] some peculiarities are still a subject of debate [15].

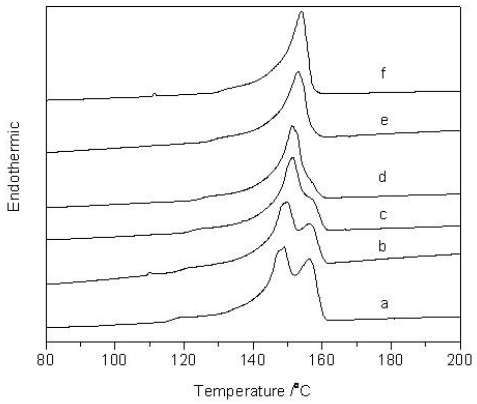

Fig. 4. Melting thermograms (β = 10 °C/min) of PP/Cloisite (C93A) 1% wt nanocomposite prepared by latex technique crystallized at different T_c: a) 385 K, b) 388 K, c) 391 K, d) 394 K, e) 397 K and f) 400 K [71]

The equilibrium melting temperature (T_m^o) is an important thermodynamic parameter for determining the degree of undercooling, which signifies the kinetic driving force for crystallization of a crystallizable polymer. It is simply said that no crystallization can occur at temperatures greater than the T_m^o. Theoretically, T_m^o is defined as the melting temperature of an infinitely large stack of extended-chain crystals in the directions perpendicular to the chain axis and with the chain ends establishing an equilibrium state of pairing [72]. From the relationship between the observed melting temperature, T_m and the crystallization temperature, two extrapolative methods can be used: (1) the linear Hoffman-Weeks (LHW) and (2) non-linear Hoffman-Weeks (NLHW), respectively.

From DSC scans (isothermal crystallization at given T_c and then melting of the crystallized sample), Hoffman and Weeks [73] proposed a method for determining the T_m^o, which states a finite linear relationship between the observed melting temperature, T_m and the crystallization temperature T_c, according to the following equation:

$$T_m = \frac{T_c}{2\gamma} + T_m^o \left[1 - \frac{1}{2\gamma}\right] \tag{14}$$

where γ is the ratio of the thickness of the mature crystals to that of the initial ones or the thickening ratio. Due to the suggested linearity of the $T_m - T_c$ data in equation, this approach will be referred to as the linear Hoffman-Weeks extrapolative method (LHW). According to this method, T_m^o is the point of intersection of T_m versus T_c straight line with the straight line that has equation, $T_m = T_c$. The polymer melting temperature increases linearly as crystallization temperature is increased [6].

Long range extrapolates causes discrepancies in literature data for the equilibrium melting temperatures of iPP: from 457.4 K [74] to 481 K [54] for α phase and 449 K for β-phase of iPP with high isotacticity content are observed. The equilibrium melting temperature of 457 K for iPP and lower values for iPP in glass-fiber composites as the content of glass fibers in the model composites increases are observed [23]. Since the equilibrium melting point decreases in iPP/fiber composites, it can be concluded that increasing the filler content increases the number of defects between iPP lamellae. This is confirmed by the higher γ values found for all composites. A large γ value is indicative of the existence of more perfect crystals, resulting from an annealing effect at the examined T_c [52].

Acknowledgments: This work was supported by the Ministry of Education and Science of R. Macedonia and COST Action P12.

REFERENCES

[1] M. Di Lorenzo, C. Silvestre, *Prog. Polym. Sci.*, **24** (1999), 917–950.

[2] B. Monasse, J. M. Haudin, *Colloid Polym. Sci.*, **264** (1986), 117–122.

[3] A. Ziabicki, *Appl. Polym. Symp.*, **6** (1967), 1–18.

[4] T. Ozawa, *Polymer*, **12** (1971), 150–158.

[5] A. Jeziorny, *Polymer*, **19** (1978), 1142–1144.

[6] P. Thanomkiat, R. A. Philips, P. Supaphol, *Eur. Polym. J.*, **40** (2004), 1671–1682.

[7] D. Park, I. Kim, Y. Han, S.D. Seul, B.U. Kim, CH.S. Ha, *J. Appl. Polym. Sci.*, **95** (2005), 231–237.

[8] J. Karger-Kocsis, In Polypropylene: An A-Z reference; Kluwer Publishers: Dordrecht, 1999.

[9] M. Fujiyama, H. Inata, *J. Appl. Polym. Sci.*, **85** (2002), 1851–1857.

[10] E. B. Bond, J. H. Spruiell, J. S. Lin, *J. Polym. Sci. Part B: Polym. Phys.*, **37** (1999), 3050–3064.

[11] P. S. Dai, P. Cebe, M. Capel, *J. Polym. Sci. Part B: Polym. Phys.*, **40** (2002), 1644–1660.

[12] J. T. Xu, F. X. Guan, T. Yasin, Z. Q. Fan, *J. Appl. Polym. Sci.*, **90** (2003), 3215–3221.

[13] M. Gahleitner, C. Bachner, E. Ratajski, G. Rohaczek, W. Neissl, *J. Appl. Polym. Sci.* **73** (1999), 2507–2515.

[14] J. Kotek, I. Kelnar, J. Baldarian, M. Raab, *Eur. Polym. J.*, **40** (2004), 2731–2738.

[15] G. Bogoeva-Gaceva, A. Janevski, A. Grozdanov, *J. Appl. Polym. Sci.*, **67** (1998), 395–404.

[16] B. Wulfhorst, G. Tetzlaff, R. Kaldenhoff, *Chem. Text.*, **42** (1992), 10–11.

[17] E. Mäder, G. Hofmann, U. Engelmann, *Proceedings of 6th International Techtextile Symposium*, **1** (1994), 327–328.

[18] S. Ramakrishna, *J. Compos. Mater.*, **31** (1997), 52–70.

[19] F. Hoecker, J. Karger-Kocsis, *J. Adhes.*, **52** (1995), 81–100.

[20] M. Avella, E. Martuscelli, C. Sellitti, E. Garagnani, *J. Mater. Sci.*, **22** (1987), 3185–3193.

[21] A. Janevski, G. Bogoeva-Gaceva, E. Mader: *J Appl. Polym. Sci.*, **74** (1999), 239–246.

[22] G. Bogoeva-Gaceva, B. Mangovska, E. Mäder, *J Appl. Polym. Sci.,* **77** (2000), 3107–3118.

[23] G. Bogoeva-Gaceva, A. Janevski, E. Mäder, *J. Adhesion Sci. Technol.*, **14, 3** (2000), 363–380.

[24] T. W. Chou, (Ed.), *Materials Science and Technology*, Vol. 13, VCH, Weinheim, 1993.

[25] B. Wunderlich, *Macromolecular Physics*, Vol. 2, Chap. 5, Academic Press, New York, 1976.

[26] A. Grozdanov, G. Bogoeva-Gaceva, M. Avella, *J. Serb. Chem. Soc.*, **67,** 12 (2002), 843–859.

[27] A. Janevski, G. Bogoeva-Gaceva, *J. Appl. Polym. Sci.*, **69** (1998), 381–389.

[28] D. S. Achilias, G. Z. Papageorgiou, G. P. Karayannadis, *Macromol. Chem. Phys.*, **206** (2005), 1511–1519.

[29] R. J. Young, P. A. Lovell, *Introduction to Polymers*, Chapman&Hall (2nd Ed.), London, 1996.

[30] R. J. Young and P. A. Lovell, A. Martinelli, L. D'Ilario, R. Caminiti, *J. Polym. Sci. Part B: Polym. Phys.*, **43** (2005), 2725–2736.

[31] P. Supaphol, J. E. Spruiell, *Polymer*, **42** (2001), 699–712.

[32] J. M. G. Cowie in: Polymers: Chemistry & Physics of Modern Materials, London, 1973.

[33] A. Keller, H. W. H. Kolnaar, Flow Induced Orientation and Structure Formation, in: *Processing of Polymers*, H. E. H. Meijer (Ed.), Vol. 18, VCH, Weinheim, Germany, 1997.

[34] O. Lee, M. R. Kamal, *Polym. Eng. Sci.*, **39** (1999), 236–248.

[35] G. Kumaraswamy, G. A. Issaian, J. A. Kornfield, *Macromolecules*, **32** (1999), 7537–7547.

[36] D. R. Rueda, F. Ania, F. J. Balta-Calleja, *Polymer*, **38** (1997), 2027–2032.

[37] I. Dukovski, M. Muthukumar, *J. Chem. Phys.*, **118** (2003), 6648–6655.

[38] M. Seki, D. W. Thurman, J. P. Oberhauser, J. A. Kornfield, *Macromolecules*, **35** (2002), 2583–2594.

[39] A. Nogales, B. S. Hsiao, R. H. Somani, S. Srinivas, A. H. Tsou, F. J. Baltá-Calleja, T. A. Ezquerra, *Polymer*, **42** (2001), 5247–5256.

[40] W. Hu, D. Frenkel, V. B. F. Mathot, *Macromolecules*, **35** (2002), 7172–7174.

[41] F. Gu, H. Bu, Z. Zhang, *Macromolecules*, **33** (2000), 5490–5494.

[42] M. J. Hill, P. J. Barham, A. Keller, *Colloid Polym. Sci.*, **258** (1980), 1023–1037.

[43] M. J. Hill, P. J. Barham, A. Keller, *Colloid Polym. Sci.*, **261** (1983), 721–735.

[44] J. D. Hoffman, J. Jr. Lauritzen, *J. Res. Natl. Bur. Stand.*, **65A** (1961), 297–336.

[45] J. Jr. Lauritzen, J. D. Hoffman, *J. Appl. Phys.*, **44** (1973), 4340–4352.

[46] J. D. Hoffman, L. J. Frolen, G.S. Ross, J. Jr. Lauritzen, *J. Res. Natl. Bur. Stand.*, **79A** (1975), 671–699.

[47] J. D. Hoffman, G. T. Davis, J. Jr. Lauritzen, The Rate of Crystallization of Linear Polymer With Chain Folding, in: *Treatise on Solid State Chemistry*, Vol. **3**, Chapter 7, N. B. Hannay (Ed.), 1976, pp. 497–614.

[48] F. C. Frank, M. Tosi, *Proc. R. Soc.*, **A263** (1961), 323–339.

[49] F. C. Frank, *J. Cryst. Growth*, **22** (1974), 233–236.

[50] S. Z. D. Cheng, B. Lotz: *Polymer*, **46** (2005), 8662–8681.

[51] J. D. Hoffmann *Polymer*, **23** (1982), 656–670.

[52] M. Avella, S. Cosco, G. D. Volpe, M. E. Errico, *Adv. Polym. Tech.* **24, 2** (2005), 132–144.

[53] J. Karger-Kocsis: Structure and morphology, in *Polypropylene: Structure, blends and composites*, Vol.1, Chapman&Hall, London, Weinheim, New York, 1995.

[54] B. Monasse, J. M. Haudin, *Coll. Polym. Sci.* **263** (1985), 822–831.

[55] G. Bogoeva-Gaceva, Lj. Raka, COST Action P12 Report 2006, http://www.uni-rostock.de/fakult/manafak/physik/poly/COST_P12/work_group_3.htm

[56] Y. Kong, J. N. Hay, *Eur. Polym. J.,* **39** (2003), 1721–1727.

[57] J. Avrami, *J. Chem. Phys.* **9** (1941), 177–184.

[58] A. Ziabicki, G.C. Alfonso, In: Memory effects in isothermal crystallization. Part I and Part II, *Colloid Polym. Sci*., **272** (1994), 1027–1042; **273** (1995), 317–323.

[59] G. Bogoeva-Gaceva, A. Grozdanov, *J. Serb. Chem. Soc*., **71** (1) (2006), 483–499.

[60] Y. Kong, J. N. Hay, *Polymer*, **43** (2002), 3873–3878.

[61] J. Janimac, S. Z. D. Cheng, A. Zhang, E. T. Hseh, *Polymer*, **33** (1992), 728–735.

[62] J. K. Godovsky, G. L. Slonimsky, *J. Polym. Sci., Polym. Phys.*, **12** (1974), 1053–1080.

[63] H. Heyns, S. Heyez, Procedings in Third Int. Conf. Therm. Anal., **3** (1971), 341.

[64] C. F. Pratt, S. Y. Hobbs, *Polymer* **17** (1976), 12–16.

[65] M. Avella, E. Martuscelli, M. Pracella, *J. Therm. Anal.*, **28** (1983), 237–248

[66] H. J. Tai, W. Y. Chiu, L. W. Chen, L. H. Chu, *J. Appl. Polym. Sci.*, **42** (1991), 3111–3122.

[67] J. H. Griffith, B. G. Rånby, *J. Polym. Sci.*, **38** (1959), 107–116.

[68] G. Guerra, V. Petracone, P. Corradini, C. De Rossa, R. Napolitano, B. Piorozzi, *J.Polym. Sci. Polym. Phys.* Ed. **22** (1984), 1029–1039.

[69] V. Petracone, G. Guerra, C. De Rossa, A. Tuzu, *Macromolecules*, **18** (1983), 813–814.

[70] V. Petracone, G. Guerra, C. De Rossa, A. Tuzu, *Macromol. Chem. Rapid Commun*., **5** (1984), 631–634.

[71] L. Raka, B. Dimzoski, J. Loos, G. Bogoeva-Gaceva, Nonisothermal and isothermal crystallization of PP/nanocomposites: Kinetic Approach, *Proceedings of European Discussion Meetings EDM 2007 on Polymer Crystallization,* Waldau, Germany, 2007, BP-26.

[72] H. Marand, J. Xu, S. Srinivas, *Macromolecules*, **31** (1998), 8219–8229.

[73] J. D. Hoffman, J. J. Weeks, *J. Res. Natl. Bur. Stand. A*, **66** (1962), 13–28.

[74] H. S. Bu, S. Z. D. Cheng, B. Wunderlich, *Macromol. Chem. Rapid Commun*., **9** (1988), 76–77.

Р е з и м е

КРИСТАЛИЗАЦИЈА НА ПОЛИПРОПИЛЕН: ПРИМЕНА НА ДИФЕРЕНЦИЈАЛНА СКЕНИРАЧКА КАЛОРИМЕТРИЈА

I. ИЗОТЕРМНА И НЕИЗОТЕРМНА КРИСТАЛИЗАЦИЈА

Изложени се теоретските основи на кристализацијата на изотактичен полипропилен со осврт на можностите на методот на диференцијалната скенирачка калориметрија, применет за анализа на изотермните и неизотермните процеси на кристализација.

Клучни зборови: полипропилен; изотактичен; кристализација; изотермна; неизотермна; диференцијална скенирачка калориметрија (ДСЦ)

Adress:
Luljeta Raka
Faculty of Natural Sciences and Mathematics, State University of Tetovo,
MK– 1200 Tetovo, Republic of Macedonia
luljeta.raka@unite.edu.mk

Gordana Bogoeva-Gaceva
Faculty of Technology and Metallurgy, University „Ss. Cyril and Methodius”,
16 Rudjer Bošković, MK–1000 Skopje, Republic of Macedonia,
gordana@tmf.ukim.edu.mk

Received: 13. XII 2007
Accepted: 28. V 2008